Iterative Rational Krylov Algorithm (IRKA) for Modelling Dynamic Temperature Distribution in Epidermal Temperature Sensors

By

Faiza Tasneem

MS-CS&E 2020 00000326119

Supervisor

Dr. Usman Khan

Co-Supervisor

Dr. Mian Ilyas Ahmad

A thesis submitted in partial fulfillment of the requirements for the degree of Masters of Science in Computational Science and Engineering (MS-CS&E)

In

School of Interdisciplinary Engineering and Sciences,

National University of Sciences and Technology (NUST),

Islamabad, Pakistan.

(September, 2023)

THESIS ACCEPTANCE CERTIFICATE

Certified that final copy of MS/MPhil thesis written by **Ms. Faiza Tasneem** Registration No.
00000326119 of ___ **SINES** ___ has been vetted by undersigned, found complete in all aspects as
per NUST Statutes/Regulations, is free of plagiarism, errors, and mistakes and is accepted as
partial fulfillment for award of MS/MPhil degree. It is further certified that necessary
amendments as pointed out by GEC members of the scholar have also been incorporated in the
said thesis.

Signature with stamp: _____

HoD ICS
SEECS-NUST
Sector H-12 Islamabad

Name of Supervisor: __Dr Usman Khan__

Date: __27-9-2023__

Signature of HoD with stamp: _____

Date: __2 8 SEP 2023__

Dr. Mian Ilyas Ahmad
HoD Engineering
Professor
SINES - NUST, Sector H-12
Islamabad

Countersign by

Signature (Dean/Principal): _____

Date: __2 8 SEP 2023__

Dr. Hammad M. Cheema
Principal & Dean
SINES - NUST, Sector H-12
Islamabad

i

Approval

It is certified that the contents and form of the thesis entitled "**Iterative Rational Krylov Algorithm (IRKA) for Modelling Dynamic Temperature Distribution in Epidermal Temperature Sensors**" submitted by **Faiza Tasneem** have been found satisfactory for the requirement of the degree.

Advisor: **Dr. Usman Khan**

Signature: _____

Date: _____

Co-Supervisor: **Dr. Mian Ilyas Ahmad**

Signature: _____

Date: _____

Committee Member 1: **Dr. Absaar ul Jabbar**

Signature: _____

Date: _____

Committee Member 2: **Dr. Salma Sherbaz**

Signature: _____

Date: _____

- to my beloveds *Mama, Baba & Mimi*

Certificate of Originality

I hereby declare that this submission is my own work and to the best of my knowledge it contains no materials previously published or written by another person, nor material which to a substantial extent has been accepted for the award of any degree or diploma at at School of Interdisciplinary Engineering and Sciences (SINES) or at any other educational institute, except where due acknowledgement has been made in the thesis. Any contribution made to the research by others, with whom I have worked at School of Interdisciplinary Engineering and Sciences (SINES) or elsewhere, is explicitly acknowledged in the thesis. I also declare that the intellectual content of this thesis is the product of my own work, except for the assistance from others in the project's design and conception or in style, presentation and linguistics which has been acknowledged.

Author Name: **Faiza Tasneem**

Signature: _____

Acknowledgments

I want to extend my sincere gratitude to everyone who helped my master's dissertation be completed successfully. This accomplishment would not have been achieved without their assistance, direction, and encouragement.

I must start by saying that my supervisor Dr. Usman Khan (SEECS) and co-supervisor Dr. Mian Ilyas Ahmed, whose support and insightful assistance were indispensable throughout the journey, deserve the ample amount of gratitude. Their knowledge, tolerance, and dedication to my learning development have been genuinely encouraging. The insightful feedback, helpful criticism, and constant support have greatly influenced the end result of this dissertation, and I am grateful for all of it. I would also like to acknowledge my GEC members Dr. Absaar Ul Jabbar for his invaluable contribution and Dr. Salma Sherbaz for her advice and kind support.

Last but not the least my loving parents, who are the reason for all of my successes and my siblings, for their never-ending support and love, deserve nothing less than my sincerest appreciation.

<u>**Faiza Tasneem**</u>

List of Abbreviations And Notations

FOM	Full Order Model
ROM	Reduced Order Model
MEMS	Micro-electromechanical Systems
TCR	Temperature Coefficient Resistance
LTI	Linear time invariant
SISO	Single Input Single Output
MIMO	Multiple Input Multiple Output
MISO	Multiple Inputs Single Output
IRKA	Iterative rational Krylov algorithm
FEA	Finite Element Analysis
FDM	Finite Difference Method
$\in$	Belongs to
:=	Equal by definition
$\mathcal{R}$	Set of all real
$\mathcal{R}^n$	Set of all real vectors of size $n \times 1$
$\mathcal{R}^{n \times m}$	Set of all real matrices of size $n \times m$
colsp	Column span
s_k	kth pole
$G(s)$	Transfer function with respect to s $\in \mathcal{C}$
$G'(s)$	Derivative of transfer function G(s) with respect to s
$\| \cdot \|_{\mathcal{H}_2}$	H_2 norm

Contents

CONTENTS

List of Figures

List of Tables

Abstract

Accurate skin temperature measurement can offer clinically useful data regarding cardiovascular health, cognitive function, cancer risk, and many other aspects of human physiology together with other measurements [36]. Skin thermometry has several uses in medicine, athletics, and research. Subsequently understanding the skin structure and its response to diverse sorts of signals is essential to design efficient and robust skin sensors. There are various devices available for skin temperature measurement for example contact thermometers, infrared cameras, surface probes and others but they offer limitations like discomfort, thermal loading, limited accuracy, one-point measurement, longer response time, are invasive and others. Epidermal sensors are a type of non-invasive wearable sensors that are designed to be placed onto the skin's surface, and are flexible, thin, that are attached to the skin like a temporary tattoo or bandage without any thermal and mechanical burden. They utilise temperature coefficient of resistance (TCR) to monitor temperature of the human skin. The TCR sensor comprises gold elements encapsulated between two layers of polyimide thin films integrated onto a thin elastomeric sheet. The design of a high performance TCR sensor requires modelling of temperature distribution and the response time. Analytical solutions of partial differential equations (PDEs) are only available for simple geometries while for complex structures like the TCR sensor numerical approach (finite difference/finite element) for solving the governing equation is used. Though finite element method (FEM) simulations provide an effective tool for modelling purposes, they are computationally complex, in particular, for spatial mapping of temperature using sensor arrays. Therefore, for an effective and time-efficient design of TCR sensors, model order reduction (MOR) of the heat equation offers an alternative approach. Here, in order to circumvent the challenge, we propose Iterative Rational Krylov Algorithm (IRKA) based MOR for modelling the temperature distribution and the time response of the epidermal TCR sensors. The comparison with

FEM simulations reveals that the IRKA based MOR offers similar accuracy with much lower computational cost as it remarkably computes the temperature distribution in a 3 orders of magnitude lesser time than the FEM simulations. IRKA based modelling of the temperature dynamics presents a promising approach for time efficient design of epidermal TCR sensors for biomedical applications.

Introduction and motivation

THE application of order reduction of the mathematical model to automatically create an accurate compact model of the epidermal temperature sensor named as TCR device is presented in this research. The lower order model produces results that are comparable to those of the original model and can be converted into a hardware description language for use directly in system-level simulation.

1.1   Epidermal sensors

The small wearable devices are remotely utilized gadgets attached to any individual to measure physiological parameters of interest. These devices can be classified in to two following categories:

1. Wearable Devices as Accessories: e.g. smart watches, smart glasses, smart clothing, wearable cameras and more.

2. Wearable Devices as Implants: e.g. skin inspired sensors, smart tattoos, healing chips, cyber pills and more.

These are externally near fitted sensors to an individual and work in both wired and remote ways. A single wearable sensor measures more than one physiological parameter, for example, the wrist monitor measures the heart rate, blood weight, and body temperature of the individual wearing it. [36] One of the essential goals of utilizing these wearable sensors is to minimize the unsettling influence confronted by the individual wearing it. Distinctive wireless technologies work alongside these sensors for real-time

data collection.

Skin is the biggest organ of human body which inherits the property to resist and secure the body from the outside world. Subsequently understanding the skin structure and its response to diverse sorts of sensing is essential to remove the scientific barriers that are preventing our capacity to design more efficient and robust skin sensors. A class of wearable, hair-thin, skin-soft, stretchable sensors and electronics having the capability of continuous and long-term physiological sensing with minimal thermal loading is named as 'Epidermal Sensors'. These sensors are integrated into adaptable and stretchable films, patches or bandages which collect the information observing crucial parameters, patient abnormalities needed for various types of treatments. Skin temperature is a vital physiological parameter having several uses in medicine, athletics, and research and its measurement can reveal important information about an individual's well-being, comfort, and performance [36]. Subsequently understanding the skin structure and its response to diverse sorts of signals is essential to design more efficient and robust skin sensors. There are various devices available for skin temperature measurement for example contact thermometers, infrared cameras, surface probes and others but they offer limitations like discomfort, thermal loading, limited accuracy, one-point measurement, longer response time, are invasive and others [25][41]. The development of such sensors has revolutionized the world of healthcare industry in many ways, for example, the doctors can monitor their patients' health and speed of recovery remotely making healthcare predictable, safe and efficient.

1.2   Problem set-up

In this thesis a Temperature Coefficient Resistance (TCR) device consisting of 16 gold elements which are used to measure human body temperature and other physical parameters i.e hydration level of skin is discussed. The primary benefit of these TCR devices is that they offer mapping capabilities rather than a single point measurement with more precision. To represent the heat transport in the skin and its impact on the sensor, these interactions can be characterised using differential equations, such as the heat conduction equation [34]. The Physical phenomenon gets the shape of the partial differential equations (PDEs) when modelled, for complicated systems, numerical simulations are helpful because analytical solutions are only feasible for simple geometries.

Numerical techniques like finite difference method (FDM) or finite element (FEM) approaches are used to solve the heat equation for predicting sensor's response time (The amount of time it takes for the sensor to increase the temperature by 90%) that plays an important role in optimising design strategy and characterisation. But the discretization resulting from FDM/FEM is too large, consisting of thousands of degrees of freedom (DoFs), hence making the computation expensive. When FEM was performed by utilising multi-physics software package COMSOL on the TCR sensor simulation took a good amount of time to provide the sensor's response (discussed in detail in section 3). This can be exhausting for the designers and engineers to quickly prototype and iterate on design in the development process. To decrease this computational work, reduction of the full order model to the lower dimension can play a crucial role. There are many physical domains including micro-electromechanical systems (MEMS) where it can be used to generate reduced models by utilising less computational resources and giving faster results [19][21][16]. Nevertheless, no efforts to apply MOR to the TCR sensor have been made so far.

1.3   Model order reduction framework

In today's world, mathematical models are typically used to describe both natural and artificial processes. These models can be used to simulate the behavior of the relevant processes. They are generally used to monitor or manage the behavior of dynamic processes since their present behavior indicates how they will behave in the future. The demand for more precision in this framework is constantly growing and hence resulting in models that are quite complicated. However, it is not always possible to simulate the entire complex model, as a result, a suitable reduction of the model is required. System approximation is mostly required in order to create simpler dynamical systems models that capture the essential components of the original complicated model. The requirement is driven by restricted computing, precision and issues like storage capacity. The reduced model is used instead of the complicated model for *system-level simulation* or *control* [28]. Model complexity can reach tens of thousands or even hundreds of thousands of degrees of freedom, as measured by the quantity of associated first order difference equations. Discretization can result in higher orders, especially in

circumstances resulting from partial differential equations (PDEs) that occur in three spatial dimensions. This complexity may cause three issues: storage, accuracy, and computing speed. In these cases, smaller simulation models are crucial for forecasting timeliness and quality. There are two more restrictions in our approach, firstly, in addition to being efficient, the algorithm must deliver an answer in a limited amount of time, and secondly, the solution must be difficult enough to be sufficiently accurate.

Model order reduction (MOR) was developed in the domain of systems and control theory, which studies properties of dynamical systems in application for reducing their complexity, while preserving input output behaviours as much as possible. MOR is an automatic process which takes a dynamic model of high order 10^2 to 10^9 and simplifies it within an acceptable amount of time and limited storage capacity but with reliable outcome. MOR tries to quickly capture essential features of the system such that the important basic properties of the original model must be present in the smaller approximation with sufficient precision [26]. The entire reduced model can be swapped out for the original model, and it can be used repeatedly throughout the design process to further cut down on time. Figure 1.1 explains the idea in graphical easy-to-understand
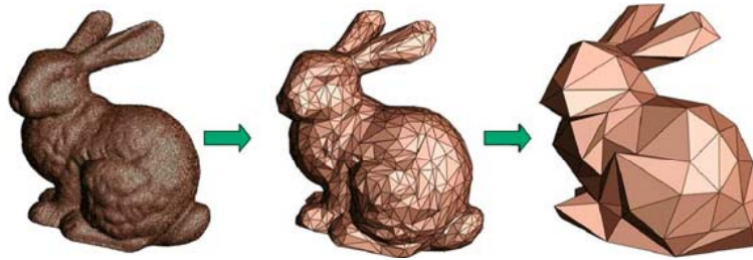
Figure 1.1: Graphical illustration of model order reduction.

way, demonstrating that typically less data is required to explain a model. This illustration using images of the Stanford Bunny demonstrates how the rabbit can still be recognised despite having only a few facets and explains how model order reduction works. (Graphics credits: Harvard University, Microsoft Research) [27].

There are numerical techniques such as finite element method (FEM) and finite difference method (FDM), which can convert continuous dynamic systems, linear and non-linear, with infinite degrees of freedom to discrete finite dimensional models. But still the resulting number of DoFs is too large, the reduction of original system size can drastically reduce the computational work. The generic framework of MOR can be represented by following flow diagram:
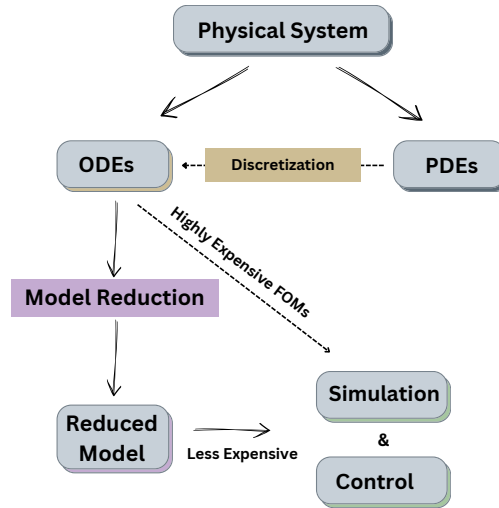
Figure 1.2: MOR Flowchart

The goals of MOR can briefly be stated as:

1. Good approximation with minimum error

2. Preservation of stability and system properties

3. Computationally stable and efficient

It is important to know that compact models, also known as lumped element models or macro models, depict how devices or systems work using a limited number of set variables. There are different approaches for creating such compact models, however, this 'classical compact modelling' is not automatic and the designer has to perform a time-consuming parameter extraction. On the other hand, the governing PDE systems are formally converted to low-dimensional standard equation systems by model order reduction (MOR), which is formal, reliable, and automated [21].

Nevertheless, to yet, there have been no attempts to apply model order reduction to TCR devices. Order reduction techniques were formerly restricted to electrical circuits and structural mechanics issues.

1.4 Motivation and scope

To make the work of designers and engineers easier, several physical, chemical, and other processes are frequently simulated on computers. Modern items can be designed in this

fashion more quickly, more consistently, and without having to create pricey prototypes. The rise in computer power is a key factor in enabling the sophisticated simulations run today. As computers and processors become faster, the increase in processing capability correlates with improvements in numerical algorithms. The main cause of this speedup in algorithms is the use of iterative solutions for linear systems. The huge speedup made possible by computer processors and algorithms has allowed computational science to advance significantly.

Due to the high complexity, small size and weight of epidermal sensors, the modelling and numerical simulation cannot be ignored for predicting device behaviour and optimising its performance [34]. Such small models in structure are complex when analysed numerically, the computational complexity increases and it becomes more expensive when analysis performed is transient. However numerical treatment of PDEs of many interconnected devices with each exhibiting a complex behaviour is expensive without the reduction of the order of the unknowns to a lower dimensional system [19]. Since these sensors frequently consist of linked components, like array structures, it is preferable to minimize each component separately before coupling them all together. Model order reduction has been the subject of extensive research in more recent years and has been a great tool to provide us a digital twin for real-time and efficient design and control. There are many physical domains like mechanical, electrical, thermal, fluid, acoustics, electromagnetism etc where it can be used to generate ROMs by utilizing less computational resources and giving faster results.

1.5 Structure of thesis

The remaining part of the thesis is structured as follows: Chapter 2 describes the Dynamic simulations of TCR device, the physical model is explained briefly and presents the literature about model order reduction. Chapter 3 discusses different techniques of reduction for LTI systems while in Chapter 4, our chosen algorithm IRKA is applied on TCR device and results comparison between Finite element (FEM) results and MATLAB are explained in chapter 5. The conclusion is summarised in chapter 6.

CHAPTER 2

Literature review

Dynamic simulation of epidermal temperature sensor

Designing modern micro-electro-mechanical systems and components such as thermal actuators, sensors and many others devices heavily relies on thermal control. We can predict the performance, reliability, and output of these systems after a thorough investigation of temperature changes in those systems. This chapter's major objective is to provide a broad overview of methods for solving the partial differential equation for heat transfer.

2.1   Physical model

Stretchable epidermal sensors developed by Webb et al. [31] act as a heating element at the same time as it is composed of gold that has been lithographically defined into intertwined serpentine traces that are 20mm long and 50nm thick. The ability to measure temperature is based on changes in electrical resistance. A top layer of PI surrounds this sensor, and another layer of PI is located underneath the sensor. A substrate made of elastomeric solaris is attached to the sensor implanted in the film [35]. The prototype of the said device as explained by [8] can be shown in Figure 2.1 with its expanded view in Figure (2.1) :

This framework comprises of 16 such sensors (each 1 mm × 1 mm) in a 4×4 layout that depend on temperature coefficient of resistance and are designed for external addressing for information acquisition, this sensor is also called as Temperature Coefficient
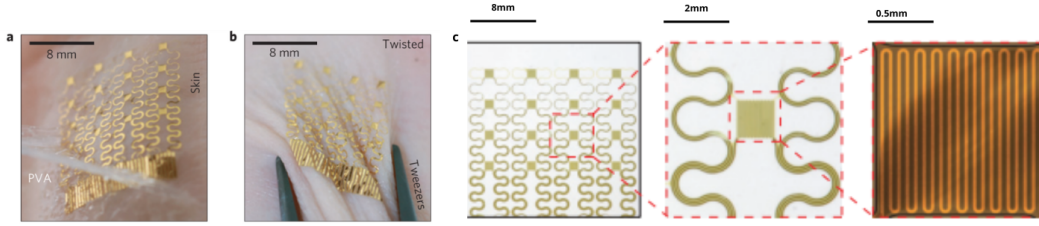
Figure 2.1: (a) Image of a 4x4 sensor array after application to the skin. (b) Similar device but deformed. (c) Enlarged views of a single sensor integrated into optical images of a 44 array sensor arrangement on a thin elastomeric substrate.

Resistance (TCR) device.[31] The two main features of TCR device are:

1. Measuring temperature through temperature coefficient of resistance α from the gold traces.

2. External addressing for transmitting information.

The relation between temperature and electrical resistance can be represented by the following expression.

$$R_t = \quad R_o(1 + \alpha \Delta T)$$

$$\alpha = (R_t - R_o)/R_o \Delta T$$

Where α represents the coefficient of change in resistance per degree of temperature change. They also experience some degree of resistance change with temperature, similar to all materials that have a specified resistance (at 20°C).This factor is positive for pure metals, indicating that resistance rises with rising temperature. When this coefficient is negative, as it is for the elements germanium, silicon, and carbon, the resistance falls as the temperature rises.

2.2 Thermal modelling of the epidermal TCR sensor

The TCR device is relatively thin and the heat flux is along thickness direction. According to [40], when the lateral sizes are much larger than thickness (1mm x 1mm x 50nm) 1D heat conduction can be adopted such that one-dimensional heat transfer model can then represent the temperature increase T (from the ambient temperature) in the film and substrate [36].

$$\frac{\partial T}{\partial t} = \alpha \frac{\partial^2 T}{\partial x^2} \tag{2.2.1}$$

where the origin is at the top of the polyimide film, x is a coordinate in the direction of thickness, and α represents thermal diffusivity.

The Physical phenomenon get the shape of the partial differential equation when modelled, numerical simulations are useful for investigating complicated systems because analytical solutions are only available for simple geometries. Figure 2.2 exhibits a cross-sectional view of the epidermal sensor.

In order to measure temperature change accurately, the response time must be as
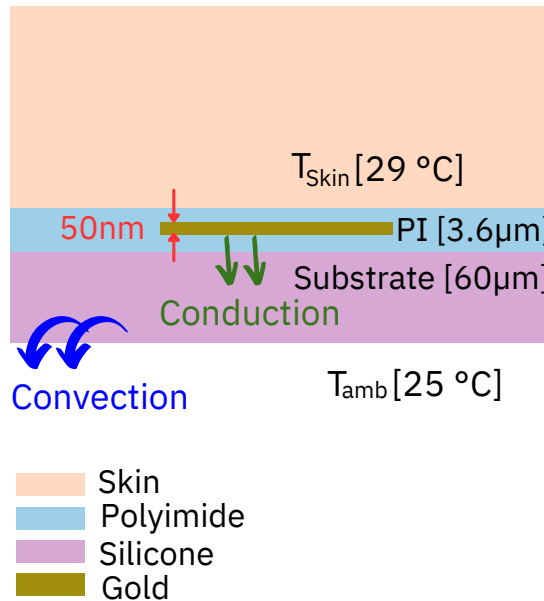
Figure 2.2: Cross-section of the TCR sensor.

short as possible (below 1 Hz), depending on the material and geometric properties. A numerical approach (FDM) for the thermal response is created (chapter 4) to help with a better understanding of how the device operates as well as the identification of new device designs and fabrication techniques.

The heat transfer equation is coupled with additional partial differential equations that are already present at the device level in the general case. Since the device is frequently surrounded by moving fluid (either gas or liquid), the Navier-Stokes equations frequently take the heat transfer in the flowing fluid into account. Because they can be connected with equation (2.2.1) to model the total heat transport, the final set of equations is exceedingly complex. By using the convective boundary condition it can be decoupled in some circumstances (as in our case) mentioned in [36].

2.3 Dynamic compact thermal modelling

Model complexity can reach tens of thousands or even hundreds of thousands of degrees of freedom, as measured by the quantity of linked first-order differential or difference equations. The complexity may lead to three problems: storage, accuracy, and processing speed, particularly in scenarios involving dynamical PDEs. Smaller simulation models are essential in these situations for predicting quality and timeliness. Since (2.2.1) is so large, as was already indicated, the simulation takes a while. The order of the resulting thermal ODE system surpasses 100,000 for a range of micro-electro mechanical systems. Because using these models during system-level simulation is impractical, accurate dynamic compact thermal models (DCTM) must be used instead. Three categories can be made out of the methods used to create DCTM: manual methods, semi-manual methods, which include modal approaches, and fully automatic methods for model order reduction. Our thesis' major topic, the automatic approach, will be covered in detail in chapter 3 using a variety of techniques. The only class of DCTM procedures that can be totally automated, or with the least level of designer intervention, is mathematical model order reduction (MOR) approaches. Hence, they are becoming more and more popular among designers of microelectronic and MEMS devices [17].

2.3.1 Model order reduction structure

By taking into consideration the state space model of a system described in the Time-Domain Approach, the idea of MOR may be comprehended as: [27].

$$\mathbf{E}\dot{x}(t) = \mathbf{A}x(t) + \mathbf{B}u(t)$$
$$y(t) = \mathbf{C}x(t) + \mathbf{D}u(t)$$
(2.3.1)

where $\mathbf{E}$, $\mathbf{A} \in \mathbb{R}^{n \times n}$, $\mathbf{B} \in \mathbb{R}^{n \times m}$, $\mathbf{C}^T \in \mathbb{R}^{p \times n}$ and $\mathbf{D} \in \mathbb{R}^{p \times m}$.

In the above equation $x(t) \in \mathbb{R}^n$ are the states and its elements are referred to as 'state variables', $u(t) \in \mathbb{R}^m$ is the input and $y(t) \in \mathbb{R}^p$ is the output vector. For the modelling purposes of LTI system here it is assumed that $\mathbf{E}$ is non-singular (i.e identity matrix) and there is no non-linearity i.e $\mathbf{D} = \mathbf{0}$. After applying reduction this system will change into following system with less number of states:

$$\dot{x}_r(t) = \mathbf{A}_r x(t) + \mathbf{B}_r u(t)$$
$$y_r(t) = \mathbf{C}_r x(t)$$
(2.3.2)

where $\mathbf{A}_r \in \mathbb{R}^{r \times r}$, $\mathbf{B}_r \in \mathbb{R}^{r \times m}$ and $\mathbf{C}_r^T \in \mathbb{R}^{p \times r}$ such that $r \ll n$ while the output of the reduced model is approximation of the original model, i.e. $y(t) \approx y_r(t)$.

This transformation can schematically shown by the figure below: [figure taken from [21]]
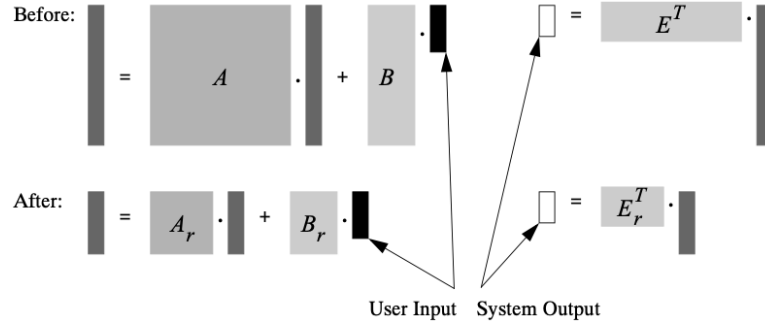
Figure 2.3: Systematic structure of reducing the dimensions of a system.

But the output of the reduced system is different from that of (2.3.1) since we incorporated the truncation error. Minimizing this inaccuracy in either the time domain or the Laplace domain is the aim of model order reduction. If we want to simulate the full network of connected devices, it is frequently impractical or even prohibitive to solve the heat transfer PDEs numerically using, for example, finite elements. Again, for a single device, the number of derived ordinary differential equations (ODEs) is easily in the 100,000 range. This enormous quantity of unknowns necessitates a lot of CPU and memory resources, even when using a parallel computing strategy for domain decomposition. Dynamic compact thermal modeling has become the industry standard for microsystem simulation because it now provides a precise and efficient solution for thermal modeling and allows for automatic system-level modeling. This is because it lowers the number of unknowns to a lower-dimensional system. To accomplish this, we have offered the well-known model order reduction techniques, which are fully automatable but, regrettably, only consider one device. Since array structures and other interconnected subsystems are common of microelectronic and MEMS devices, it is preferable, especially for devices with several sub-systems, to decouple each component and then extract a heat-transfer macro-model of it.

2.4 Linear model order reduction methods

The goal of this section is to explain a variety of relevant MOR methods for linear systems. A number of publications that introduce various approaches to the issue are presented in the literature. To get a reduced order model, most of these techniques project into lower-dimensional subspaces. The following justification is provided for this projection [28]:

- A state transformation by classifying a certain criteria, followed by a truncation of redundant information to the selected criteria. i.e. Balanced truncation

- Interpolation and moment matching approximation using Krylov subspaces.

- The forward error norm, such as the Hankel norm and the H_2 norm, should be minimized as an optimization criterion.

Since it converts the higher order model to the lower order model while essentially maintaining an assessment of all of the fundamental properties of the higher order model, system reduction is significant in the field of control system engineering [39]. The idea of reduction approach is used to generate a reduced order model by minimising the integral square impulse response error between the transient regions of the original and reduced order systems [6]. Following that, different strategies for reducing equation error were proposed based on the same notion with trade-off among some important factors including computing stability, accuracy and cost. While some of these methods, like balanced truncation and Hankel norm approximation, give a priori error bounds and guarantee stable approximations, they are computationally inefficient for large-scale systems since they necessitate the solution of Lyapunov equations. For model reduction, numerous iterative strategies based on Krylov subspaces have also been widely employed, these methods use sparsity, which is prevalent in large scale systems, due to the fact that they only require matrix-vector multiplications, they are computationally efficient [28]. Krylov based approaches have emerged as one of the most potent tools for reduced-order modelling of large-scale systems in recent years. We would like to draw the reader's attention to recent surveys on the subject [20, 13], which compliment this study. The first model order reduction technique was presented by Davison in 1966 [3]. For single input single output (SISO) systems as well as multi input multi output (MIMO) systems, a number of strategies to approximate the higher order model into a reduced order model

have been presented by researchers and are documented in the literature. The first model order reduction technique was presented by Davison in 1966 [3]; modified by Chidambara, 1967 [5, 7].

Starting from the stable linear state space form:

$$\dot{x}(t) = \mathbf{A}x(t) + \mathbf{B}u(t)$$
$$y(t) = \mathbf{C}x(t) \tag{2.4.1}$$

Where $x(t) \in \mathbb{R}^n$ is the state vector , $u(t) \in \mathbb{R}^m$ is the input signal and $y(t) \in \mathbb{R}^p$ is the output measurement vector, n is the state space dimension while m and p are the number of inputs and outputs respectively. The transfer function representation of (2.4.1) is given by:

$$G(s) = C(sI - A)^{-1}B \tag{2.4.2}$$

and the rth order transfer function of reduced system (2.4.2) that gives the original transfer function G(s) in some norm as an approximate form:

$$G_r(s) = C_r(sI_r - A_r)^{-1}B_r \tag{2.4.3}$$

The following characteristics should all be met as much as possible.

1. The forward error associated with reduced transfer function i.e. $G(s) - G_r(s)$ is small.

2. Important system properties, such as stability, are preserved.

3. The reduced system can be obtained by efficient computation.

Generally the reduced models are produced by following Galerkin methods. Let $V \in \mathbb{R}^{nxr}$ and $W \in \mathbb{R}^{nxr}$ such that $W^T V = I$. Then $V x_r(t)$ will approximate x(t) by implementing:

$$W^T(V\dot{x}_r(t) - AVx_r(t) - Bu(t)) = 0 \tag{2.4.4}$$

where $A_r = W^T AV$, $B_r = W^T B$, and $C_r = C^T V$ and column spaces of V and W span Krylov sub-spaces that minimizes the deviation of $Vx_r(t)$ from x(t) uniformly over a large set of inputs.

Before addressing different techniques, let's first analyze two crucial features of the system (2.4.4) called controllability and observability. The system is said to be controllable

if an input u(t) travels from x_0 to x_1 in a finite amount of time for any beginning state $x(t_0) = x_0$ and any final state x_1. It is observable if, over a finite time interval, any unknown initial state $x(t_0) = x_0$ can be uniquely inferred from the supplied input u(t) and the observed output y(t). The system (2.4.1) is assumed to be a so-called minimum realization in the following sections, meaning that there are no states that are neither controllable nor observable.As in the case of the MEMS case study in this thesis, a system produced by the spatial discretization of a computational domain is always a minimum realisation [21]. Controllability and the observability grammians are defined as:

$$\mathcal{P} = \int_0^\infty e^{At} BB^T e^{A^T}\, dt \tag{2.4.5}$$

$$\mathcal{Q} = \int_0^\infty e^{At} C^T C e^{A^T}\, dt \tag{2.4.6}$$

According to [21], the criterion for controllability and observability can be demonstrated by the fact that $\mathcal{P}$ and $\mathcal{Q}$ must both are of full rank. The grammians can be calculated as the singular and positive definite solutions of the following two Lyapunov equations that are part of the system as long as all of the eigenvalues of the symmetric real matrix A are positive definite and have negative real portions if $xTAx > 0 \forall x \neq 0$ (2.4.1).

$$\begin{aligned} A\mathcal{P} + \mathcal{P}A^T + BB^T = 0 \\ A^T\mathcal{Q} + \mathcal{Q}A + C^T C = 0 \end{aligned} \tag{2.4.7}$$

In order to find controllability and observability grammians, Lyapunov equations can be solved directly and in numerically stable ways [18]. Some of the well-known reduction techniques are:

2.4.1 Balanced truncation approximation

The objective of model reduction by balanced truncation when modeling a linear system is to provide a reduced order model by finding and removing/truncating those states that are simultaneously least visible and controllable. Sometimes referred to as the model's McMillan degree, the length of the state vector related to the resulting reduced order model, also known as the minimum realisation. When a model's order is more than the McMillan degree, the state vector contains one or more uncontrollable/unobservable states [20]. These gramians can be used to classify a minimal state space model according to the energy associated with each state of the system, the controllability and

observability gramians must be equal and diagonal for this implementation, but this involves a state change. A balanced realization is one that fits this description, B. C. Moore [8] was able to suggest such a similarity transformation. Hankel singular values, which are arranged in a series of progressively smaller values, are represented by the diagonal entries. This balances the system, that is, sets both gramians equal and diagonal. i.e

$$\mathcal{P} = \mathcal{Q} = diag(s_1, s_2, s_3, ..., s_n) \tag{2.4.8}$$

and $s_i \geq s_{i+1}$ for $i = 1, 2, ..., n-1$ where s_i is the ith Hankel singular value and are system characteristics that merely depend on input-output behavior. The square root of the eigenvalues of the product of grammians is used to calculate the Hankel singular values.

$$s_i = \sqrt{\lambda_i(\mathcal{P}\mathcal{Q})}, i = 1, 2, ..., n. \tag{2.4.9}$$

For any stable state space model, a non-singular transformation that yields balanced minimization is sufficient. Suppose that $G(s)$ is a stable model, It is sufficient to truncate those state variables associated with smaller Hankel singular values, removing (truncating) them from the equation. Applying a projection, such as the square-root technique, on the original system allows for simultaneous balancing and truncation, [18] discusses some other alternative algorithms which can be studied in detail. The controllability and observability gramians of reduced system $G_r(s)$ are diagonal and equal, $\mathcal{P}_r = \mathcal{Q}_r = diag(s_1, s_2, s_3, ..., s_r)$. By design, this reduced model $G(s)$ is assured to be minimum and stable, and the forward error $G(s) - G_r(s)$'s $\mathcal{H}_\infty$ norm is bounded by twice the sum of the truncated Hankel singular values [28].

$$\|G(s) - G_r(s)\|_{\mathcal{H}_\infty} \leq 2(s_{r+1}, s_{r+2}, ..., s_n) \tag{2.4.10}$$

where $\|.\|_{\mathcal{H}_\infty}$ represents the transfer function difference between the original and reduced models with the largest magnitude. The balanced truncation technique incorporates an a priori error bound and guarantees stability, but numerically it is inefficient, especially for large scale systems. The Lyapunov equation's solution is often computationally expensive, which is the primary reason of this.

2.4.2 Hankel norm approximation

The Hankel norm $\|.\|_{\mathcal{H}}$ can be defined as maximum Hankel singular value:

$$\|G(s)\|_{\mathcal{H}} = \sqrt{\lambda_{max}(\mathcal{PQ})} = s_{max} \qquad (2.4.11)$$

Finding an approximate solution $G_r^{HNA}(s)$ of degree $r < n$ is known as the optimal Hankel norm approximation problem such that the error $\|G(s) - G_r^{HNA}(s)\|_{\mathcal{H}}$ is minimized, [18] provides the lower bound for the above norm as:

$$s_{r+1} \leq \|G(s) - G_r^{HNA}(s)\|_{\mathcal{H}}$$

The above relation only holds for any G(s) with r stable poles. Since is the infinity norm is never smaller than the Hankel norm [32] so above relation can be restated as:

$$s_{r+1} \leq \|G(s) - G_r^{HNA}(s)\|_{\infty}$$

an approach for constructing an optimal Hankel norm approximation. The following upper bound is satisfied by $G_r^{HNA}(s)$ of the Hankel norm approximation of order r:

$$\|G(s) - G_r^{HNA}(s)\|_{\infty} \leq (s_{r+1} + ... + s_n)$$

which represents the bound balanced truncation technique by half.

In addition to the two methods above, a number of alternative reduction procedures suitable for linear systems are also deduced from the control theory. None of them, nevertheless, provide an estimation of the error. [11] provides an excellent overview of the methods currently in practice.

2.4.3 Moment matching approximation

Reduction of (2.4.1) by moment matching involves the confinement of some moments of $G(s)$ in the reduced order system $G_r(s)$ such that at expected interpolation points (also known as shifts) s_k in the complex plane, $G_r(s)$ interpolates the values of $G(s)$, and possibly the derivative values as well. For our purposes, easy Hermite interpolation serves the purpose, and the more moments matched the more accurate the reduced model will be, so our the main issue is to find A_r, B_r and C_r so that:

$G(s_k) = G_r(s_k) \quad$ and $\quad G'(s_k) = G_r'(s_k) \quad$ for $\quad$ k $= 1, 2, ..., r$

If the transfer function G(s) from (2.4.2) is expanded into its Taylor Series around an expansion point s_0 [21]:

$$
\begin{aligned}
G(s) &= C[(s - s_0)I - A]^{-1} - B \\
&= C[(s - s_0)I + (s_0I - A)]^{-1} - B \\
&= C[I + (s_0I - A)^{-1}(s - s_0)]^{-1}(s_0I - A)^{-1}B \\
&= \sum_{i=0}^{\infty} C[-(s_0I - A)^{-1}]^i (s_0I - A)^{-1} B (s - s_0)^i \\
&= \sum_{i=0}^{\infty} m_i(s_0)
\end{aligned}
\tag{2.4.12}
$$

where $C[-(s_0I - A)^{-1}]^i (s_0I - A)^{-1} B (s - s_0)^i =: m_i(s_0)$

For a SISO system the coefficients of $m_i(s_0)$ are known as moments of the original system's transfer function G(s).

They are matrices and are referred to as block moments if the system is multiple-input, multiple-output (MIMO), multiple-input, single-output (MISO), or single-input, multiple-output (SIMO). These moment vectors are used to construct the projection matrices, such as V and W. Moment matching properties for various scenarios are calculated using the Tylor series expansion [28].

Case I: At $s = \infty$

Let the transfer function G(s) is analytical around infinity then its Taylor series expansion: $G(s) = m_1^\infty + m_2^\infty + m_3^\infty + ...$ converges, where m_i^∞, the ith moment evaluated at infinity are known as *Markov Parameters*. Let the reduced model $G_r(s)$ has convergent series expansion that matches first 2r Markov parameters of G(s) i.e. $m_i^\infty = m_{r_i}^\infty$ for $i = 1, 2, ..., 2r$ and $r < n$, then the reduced order model is called *partial realisation* of original FOM giving better approximation at t=0 i.e. $s = \infty$.

Case II: At s=0

Tylor series expansion at s=0, can be simplified to $m_i(0) = C(A)^{-(1+i)}B$ for $i \geq 0$. This expansion around $s = 0$ is called *Pade Approximation* [34] if its series expansion has first 2r moments that satisfy $m_i^0 = m_{r_i}^0$ for $i = 1, 2, ..., 2r$

Case III: At $s = s_0$

The series expansion at a shifted frequency s_0 is given by

$$G(s) = \sum_{i=0}^{\infty} m_i^{s_0}(s - s_0)$$

involves shifted moments $m_i(s_0) = C(s_0 I - A)^{-(1+i)} B$ for $i \geq 0$. This approximation is called *Shifted Pade Approximation* where a G(s) and its 2r-1 derivatives are interpolated by ROM at predefined interpolating frequencies. Interpolation at a set of predetermined frequencies is an extension of the situation discussed above.

Case IV: At $S = \{s_1, s_2 \ldots s_k\}$

Using many expansion points and matching multiple moments for each expansion point can improve the accuracy of the single-point expansion. This multi-point approximation is called *Multi-point Pade Approximation* or *Rational Interpolation* [21][11]. Using set of distinct k interpolation points $\{s_1, s_2 \ldots s_k\}$ the ROM acquired, for instance,

$$range\{V\} = span\{B_r(s_1), B_r(s_2), .., B_r(s_k)\}$$

$$range\{W\} = span\{C_r(s_1), C_r(s_2), .., C_r(s_k)\}$$

matches the first two moments $m_0(s_i)$ and $m_1(s_i)$ for i = 1,2,...,k.

There exist implicit and explicit implementation techniques for the above problems [22] [12], but explicit moment matching techniques need to compute 2k moments for both the original and reduced system due to which they are out of condition and expensive to compute.On the other hand, Krylov-based methods achieve moment matching without explicitly computing moments [23]. Considering Krylov-based projection methods, particularly Arnoldi and Lanczos explained in [1] and [2] respectively. Because case IV cannot be solved using the standard Lanczos method, Arnoldi formula, or Block Arnoldi procedure, the subspace spanned by either W or V is no longer a Krylov subspace. The rational Krylov methods (rational Lanczos algorithm and rational Arnoldi algorithm) would be better choices.

Design and Methodology

Krylov-based techniques

The Krylov-based projection algorithms only use matrix-vector multiplications, in contrast to balanced truncation and other reduction approaches. In many cases, Krylov subspaces are excellent candidates for the desired low-order subspace of the equation, and most popular model reduction techniques for large-scale systems are Krylov based in one form or another. It should be emphasized that the Krylov subspace-based iterative methods for solving a system of linear equations are among the top 10 algorithms of the 20th century [15]. This section provides an overview of Krylov-based linear system model reduction techniques. Arnoldi and the Lanczos, two significant conventional Krylov-based algorithms that define the notion of Krylov projection in the context of model reduction by computing orthogonal and bi-orthogonal bases to the Krylov subspace, respectively:

Definition:

A Krylov subspace of kth dimension of the matrix $A \in \mathbb{R}^n \times \mathbb{R}^n$ and a vector $b \in \mathbb{R}^n$ is a subspace spanned by vector b and the vectors produced by consecutive multiplication of matrix A and vector b up to $k-1$ times, [17]

$$\mathcal{K}_r^k(A, b) = span\{b, Ab, A^2b, ..., A^{k-1}b\} \tag{3.0.1}$$

the derived vectors make a basis for k-dimensional subspace. However, if we tend to compute them directly as described, then, due to rounding errors, they'd become computationally linearly dependant even for sufficiently small k [17].

Rational Krylov method

The rational Krylov method is an extension of the Arnoldi and Lanczos algorithms and provides a satisfactory approximation at specified frequencies. The Krylov subspace associated with the shifted frequencies s and A, B can be stated as:

$$\mathcal{K}_{r_s}\left((sI-A)^{-1},(sI-A)^{-1}B\right) = \text{colsp}\left[(sI-A)^{-1}B\cdots(sI-A)^{-r_s}B\right] \quad (3.0.2)$$

In [24] it is provided that if the reduced model $G_r(s)$ interpolates the original system $G(s)$ at $-\lambda_i(A)$ and $-\lambda_i(A_r)$ then the error in $\mathcal{H}_2$ norm is small, however, $-\lambda_i(A_r)$ is not known a *priori*. But there exist an effective strategy provided by Meier and Luenberger in [4] explaining that interpolation $-\lambda_i(A_r)$ is more useful. A necessary condition for $\mathcal{H}_\in$ optimality, which can be stated in the following Lemma:

Lemma 3.1: [4, 24] Given a stable system $G(s) = C(sI-A)^{-1}B$, let $G_r(s) = C_r(sI_r - A_r)^{-1}B_r$ be a local minimizer of the dimension m for the optimal $\mathcal{H}_2$ model reduction, and suppose that $G_r(s)$ has simple poles at $-s_i, i = 1,...,r$. Then $G_r(s)$ interpolates both G(s) and its first derivative at $s_i, i = 1,...,r$:

$$G_r(s_i) = G(s_i), G_r^{'}(s_i) = G^{'}(s_i); \ \forall s_i \in S_r := s_1, s_2, ..., s_r \quad (3.0.3)$$

Recently, it was demonstrated in [24] that, for continuous time SISO systems with simple poles, the necessary optimality conditions are equal to the Meier-Luenberger conditions[4, 6]. Similar results for MIMO system are also formulated which can be found in [24, 33]. Furthermore, the rational Krylov method-based suggested iterative algorithm accomplishes moment matching and meets the interpolation-based optimality criterion upon convergence [24]. The algorithm uses rational Krylov steps to build $G_r(s)$, demonstrating its efficacy, without the need for expensive Lyapunov solvers, especially for large-scale systems. The two approaches [4, 10] rely on interpolation-based necessary conditions. The authors use the $G(s)$ and $G_r(s)$ transfer functions; iterate over the denominator or the poles and residues of $G_r(s)$; and explicitly compute G(s), $G_r(s)$, and their derivatives at specific locations in the complex plane [4, 10]. It is not preferred to work directly with the transfer function, its values, and its derivative values in large-scale contexts. Additionally, it might be extremely unsuitable to attempt to calculate the transfer function's coefficients. These methods are comparable to those in [10, 9], where transfer functions are used explicitly to perform interpolation. However, our method

is numerically stable and effective since it is based on the association between efficient rational Krylov iteration and interpolation, which is covered in more detail below.

Let s represents the collection of interpolation points $s_1, ..., s_r$. Using these interpolation points, create a reduced order model $G_r(s)$, that interpolates both $G(s)$ and $G(s)$ at $s_1, ..., s_r$. Assume $\lambda(s)$ represents the resulting poles of $G_r(s)$, Define a function $g(s)$ such that $g(s) = \lambda(s) + s$. Aside from problems with the reduced order poles' ordering, $g(s) = 0$ is equal to necessary condition for $\mathcal{H}_2$ optimality of the reduced order model [9]. The rood finding problem of $g(s) = 0$ is solved by Newton's method, which appears as several feasible solutions to this issue, and can be stated as:

$$s^{(k+1)} = s^{(k)} - (\mathbf{I_r} + \mathbf{J})^{-1} \left(s^{(\mathbf{k})} + \boldsymbol{\lambda} \left(s^{(\mathbf{k})} \right) \right) \tag{3.0.4}$$

where $\boldsymbol{J}$ represents the Jacobian of $\boldsymbol{\lambda(s)}$.

3.1 Iterative Rational Krylov Algorithm (IRKA)

Necessary optimality conditions mentioned in (3.0.3) are equivalent to root finding problem of $s_r = -\lambda(A_r)$, where λ represents eigenvalues and s_i are the required roots, this equivalence is proved in [11], pg. 10. Using Lemma 3.1 Newton iterations are used to compute the roots that successively keeps updating $s_r^{i+1} = -\lambda_i(A_r)$ [28]. The Jacobian matrix's entries often grow small in the neighbourhood of an $\mathcal{H}_2$ optimal shifts that makes it possible for setting $\boldsymbol{J} = \boldsymbol{0}$ to act as a relaxed iteration strategy. A successive substitution framework results from this i.e. $s_i \leftarrow -\lambda_i(\mathbf{A}_r)$. After convergence the necessary optimality conditions are met. The stated algorithm has been used in multiple large systems. The approach performed effectively in each of the numerical examples: It consistently converged after a limited number of steps and produced stable reduced systems. The question that emerges is whether or not this reduced order model is globally optimal in some sense, however A.C. Antoulas' work provides the solution to this problem in [24], p. 7, Theorem 3.4 and associated Corollary 3.5.

The resulting reduced model for the suggested algorithm may be influenced by the initial shift choice. Yet, a random initial shift selection produced a suitable reduced model in the majority of the cases. The method reached the global minimizer for small order benchmark instances chosen from [9][14]. The results were comparable to balanced truncation for larger problems. Consequently, we were able to get results that are on par

with or even superior to those obtained through balanced truncation while preserving a numerically effective Krylov projection framework. We offer a few initialization methods that aim to enhance the results. Remember that the eigenvalues of A_r at convergence are mirrored at the interpolation locations. Assuming convergence, interpolation points will be in the mirror spectrum of A since one can expect that the eigenvalues of A_r will be similar to those of A. As a result, one may choose initial shifts that are randomly distributed throughout a region that has the opposite numerical range of A. The $\mathcal{H}_2$ expression serves as the beginning point for another initialization strategy, where it is reasonable to begin the proposed approach with $s_i = -\lambda(A_i)$, where $\lambda(A_i)$ are the poles with big residuals ϕ_i for $i = 1, ..., r$. This approach necessitates a state-space decomposition for G(s), that will be intense to compute for complex issues. The original state-space representation may, however, be in the modal form in some applications and ϕ_i can be retrieved directly from B and C^T.

CHAPTER 4

Implementation of IRKA on the epidermal TCR sensor

Considering the detailed physical model of TCR device and the governing equation. To find out the solution of PDEs, they are first converted into ODEs by implementing any discretization scheme. There are many techniques of discretization in the literature, for example in [30] finite volume method FVM is used for structural analysis of RF mems devices, similarly in [37] the author uses finite difference method FDM for simulation of heat transfer. Here we'll discretize 1D transient heat transfer (2.3.1) using FDM and observe that how meshing effects the accuracy and computational power. Various schemes of FDM has been explored in the literature but we will be using FDM in the case of TCR device. The heat transfer equation with the initial and boundary conditions can be referred back to [36] and can be stated as follows:

$$\frac{\partial T}{\partial t} - \alpha \frac{\partial^2 T}{\partial x^2} = 0, \tag{4.0.1}$$

where the temperature rises steadily when in touch with human skin (x is the coordinate in the direction of thickness with its origin at the top) T_0:

$$T|_{x=0} = T_0 \tag{4.0.2}$$

The condition of temperature and heat flux continuity across the film/substrate contact is provided as:

Properties	Value	Descriptions
H_{film}	$3.6\mu m$	Film Thickness
H_{sub}	$60\mu m$	Substrate Thickness
H_{Au}	$50nm$	Thickness of Gold Element
w_{Au}	$1mm$	Width of Gold Element
w_{cs}	$2mm$	Width of Cross Section
α_f	$7.75 \times 10^{-8} m^2 s^{-1}$	Thermal Diffusivity of Film
α_s	$1.08 \times 10^{-7} m^2 s^{-1}$	Thermal Diffusivity of Substrate
k_f	$0.12 \times 10^{-8} W m^{-1} K^{-1}$	Thermal Conductivity of Film
k_f	$0.21 \times 10^{-8} W m^{-1} K^{-1}$	Thermal Conductivity of Substrate
h	$10\ W m^{-2} K^{-1}$	Heat Convection Coefficient

Table 4.1: List of Parameters

$$T|_{x=H_{fim}-0} = T|_{x=H_{film}+0} \text{ and } -k_{film} \left.\frac{\partial T}{\partial x}\right|_{x=H_{film}-0}$$
$$= -k_{substrate} \left.\frac{\partial T}{\partial x}\right|_{x=H_{film+0}}, \tag{4.0.3}$$

where k is the material's thermal conductivity. The natural convection at the substrate's bottom surface is described as follows:

$$k \left.\frac{\partial T}{\partial x}\right|_{x=H_{film}+H_{substrate}} = h\left(T - T_{amb}\right). \tag{4.0.4}$$

Initial condition of the system:

$$T|_{t=0} = 0. \tag{4.0.5}$$

Below in table 4.1is the list of parameters [36] that shall be used while considering the geometry and physical properties of the materials used in TCR device.

The energy balancing approach is an alternative method that may be utilized in many cases to construct the finite-difference version of equation (4.0.1). We may also use the central-difference approximations to the spatial derivatives to obtain the finite difference form of the equation. With the aid of this technique, a broad variety of phenomena can be studied, including those involving numerous materials, embedded heat sources, and exposed surfaces that don't coincide with the axes of a coordinate system.

Use of conservation of energy to a control volume surrounding the nodal region yields the finite-difference equation for a node in the energy balance approach. Because it is

frequently unknown whether heat flow is actually going into or out of the node, it is simpler to create the energy balance by assuming that all heat flow is into the node. The appropriate form of the finite-difference equation can be attained if the rate equations are expressed in a way that is consistent with this assumption, despite the fact that such a condition is obviously not conceivable. In [29] the first law of thermodynamic states that " The increase in the amount of energy stored in a control volume must equal the amount of energy that enters the control volume, minus the amount of energy that leaves the control volume". However in the case of heat transfer we focus on thermal form of energy. Because different types of energy can be transformed into thermal or mechanical energy, it's crucial to realize that the overall amount of thermal and mechanical energy is not conserved. So, the following is a statement of the first law appropriate for heat transfer analysis: *"The rate of increase of thermal energy stored in the control volume must equal the rate at which thermal energy enters the control volume, minus the rate at which thermal energy leaves the control volume, plus the rate at which thermal energy is generated within the control volume [29]"*. If we use the subscript st to indicate energy stored in the control volume and let E stand for the sum of thermal energy, then $E_s t$ will represent the change in thermal energy stored throughout the time interval t. Energy entering and leaving the control volume are indicated by the subscripts in and out. Lastly, the symbol E_g is assigned to the energy generation. The balancing of energy can expressed as follows:

$$\dot{E}_{\text{st}} \equiv \frac{dE_{\text{st}}}{dt} = \dot{E}_{\text{in}} - \dot{E}_{\text{out}} + \dot{E}_g \tag{4.0.6}$$

Keeping in view the our case of heat transfer there is no internal energy generation and no energy is leaving the system so (4.0.6) can be redefined as:

$$\dot{E}_{\text{st}} = \dot{E}_{\text{in}} \tag{4.0.7}$$

Applying equation (4.0.7) on a control volume surrounding the interior node *'i'*. Conduction between *'i'* and its two adjacent nodes affects energy exchange under one-dimensional circumstances (see the Figures 4.1) [29].
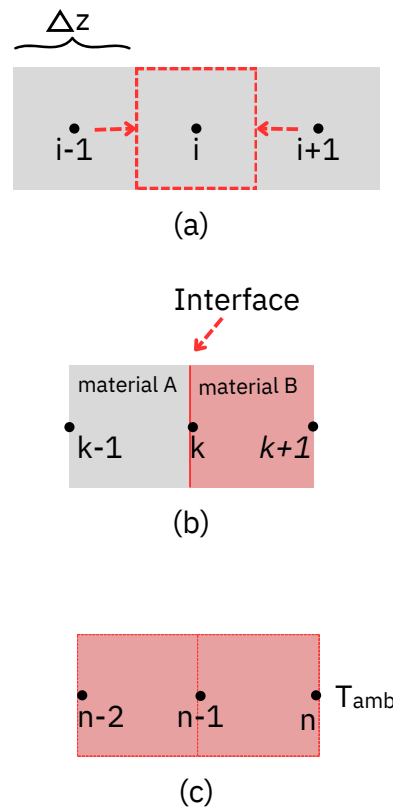
25

Figure 4.1: Discretization at (a)the contact surface with skin, (b) the interface between two materials (polyimide and sillicone) and (c) the surface exposed in air.

The overview of nodal finite difference equations for different cases i.e at interior nodes, at the interface node, and at the convective boundary node is represented respectively here:

$$\frac{\partial T_i}{\partial t} = \frac{\alpha}{(\Delta x)^2}(T_{i+1} - 2T_i + T_{i-1}) \tag{4.0.8}$$

$$\frac{\partial T_k}{\partial t} = \frac{1}{(\Delta x)^2}[k_f(T_{k-1} - T_k) + k_s(T_{k+1} - T_k) - \frac{k_f + k_s}{2}T_k] \tag{4.0.9}$$

$$\frac{\partial T_n}{\partial t} = \frac{\alpha_s}{(\Delta x)^2}[2T_{n-1} - 2\left(\frac{h\Delta x}{4k_s} + 1\right)T_n + \frac{2h\Delta x}{k_s}T_{amb}] \tag{4.0.10}$$

Considering k^{th} node at the interface. The set of equations for a single sensor gets the shape of matrices after discretization in the form of state model as described by equation (4.0.1). For more than one sensors i.e 16 in the TCR device, the representation remains same but the matrices represent block matrices.

$$A = \begin{bmatrix} \frac{-2\alpha_f}{\Delta x^2} & \frac{\alpha_f}{\Delta x^2} & & & & & & \\ \frac{\alpha_f}{\Delta x^2} & -\frac{-2\alpha_f}{\Delta x^2} & \frac{\alpha_f}{\Delta x^2} & & & & & \\ & \ddots & \ddots & \ddots & & & & \\ & & \frac{\alpha_f}{\Delta x^2} & \frac{-2\alpha_f}{\Delta x^2} & & \frac{\alpha_f}{\Delta x^2} & & \\ & & & \frac{\alpha_f}{\Delta x^2} & -(\frac{\alpha_f}{\Delta x^2} + \frac{\alpha_f}{\Delta x^2}) & \frac{\alpha_s}{\Delta x^2} & & \\ & & & & \frac{\alpha_s}{\Delta x^2} & \frac{-2\alpha_s}{\Delta x^2} & \frac{\alpha_s}{\Delta x^2} & \\ & & & & & \ddots & \ddots & \ddots \\ & & & & & 0 & \frac{2\alpha_s}{\Delta x^2} & (1 + \frac{h\Delta x}{k_s}) \end{bmatrix}$$ and

$$B = \begin{bmatrix} \frac{\alpha_f}{\Delta x^2} & 0 \\ 0 & 0 \\ \vdots & \vdots \\ 0 & 0 \\ 0 & \frac{2h\alpha_s}{\Delta x k_s} \end{bmatrix} \; ; \text{ while } u = \begin{bmatrix} T_{skin} \\ T_{amb} \end{bmatrix}$$

27

Where C can be chosen according to the requirement of output. Selection of Δx and time step i.e Δt impact the accuracy and simulation time. By lowering the values of Δx and Δt, accuracy of the finite difference solution can be increased. Naturally, as Δx decreases, more interior nodal points must be taken into account, and as Δt decreases, to bring the response to a predetermined final time, further time intervals are required. Therefore, as Δx and Δt decrease, computation time increases. The selection of Δx is frequently depending on a compromise between accuracy and processing requirements. However, once this decision is made, Δt cannot be made on its own. Instead, the requirements for stability dictate it. In a dynamic problem, the nodal temperature solution should continue increase over time as it approaches the eventual steady-state values. The required value of Δt must be kept below a predetermined limit, which depends on Δx and other system factors, to prevent the solution from deviating from the real steady-state conditions when using the explicit method, in which unknown nodal temperatures for the new time are solely determined by known nodal temperatures at the previous time. After discretizing the domain, the model was simulated in MATLAB. A table with values used for the material properties can be found above and all material properties are considered to be temperature and time independent. We take the input signal to be the skin temperature and ambient temperature u(t) while the output y(t) is the temperature of human body measured by the sensing element (gold) embedded between PI film layers. A linear thermal system with n=530 is produced by spatially discretizing the governing heat transfer equation using finite differences with restriction of $\Delta x = 0.12 \times 10^{-6}$ and the simulation time is 30ms . The restriction of choosing Δx is made here because we wanted one node at the interface of polyimide and silicon so the dicretization at that node can be defined properly. To see whether the temperature distribution that we got from the simulation of state space is correct or not, the response time i.e the time at which sensor reaches 90% of human body temperature, is cross validated with the COMSOL model and analytical results presented in [36]. Next chapter discusses the results.

Convergence of relative error

Calculating the difference between original model and reduced models with order r is perhaps the easiest method for estimating the error in the time domain or frequency domain. Relative frequency response error is defined as:

$$E_r(s) = \frac{|G(s) - G_r(s)|}{|G(s)|} \tag{4.0.11}$$

As said previously, this error indication can also be utilized in the time-domain. "Quadratic relative step-response error" shall be defined as:

$$\varepsilon(r) = \frac{1}{N} \cdot \sqrt{\sum_{t=0}^{N \cdot \Delta t} \left(\frac{y(t) - y_r(t)}{y(t)} \right)^2} \tag{4.0.12}$$

where $y(t)$ and $y_r(t)$ are the outputs of original and reduced model respectively.

CHAPTER 5

Results and Discussion

5.1 Full-order model FEM simulation results

The TCR sensor is simulated in COMSOL which is a versatile, user-friendly, and powerful multi-physics simulation tool used to accurately and efficiently simulate a variety of engineering and scientific applications by exploiting FEA. After selecting heat transfer transient study, adding parameters, creating geometry, inserting physical properties from the material library, plugging in the IC's and and BC's, the transient study was performed and computation took $\approx$ 40 min to simulate with around 68k DoFs. The results show that the sensor's response time matches with the experimental results presented in [38] i.e 3.9ms. Figure 5.1 is representing the temperature distribution on the surface of the sensor (Zoomed-in View) at the initial state and at the time of response. Figures 5.2 and 5.3 are showing the line graphs at four different points and a line defined along the sensor's cross-section. The same device was simulated after changing encapsulation of the layer from 3.6um to 6um and noticed that the response time also increased to approximately 10.2ms 5.4. Hence changing the width of layer will affect the time response.
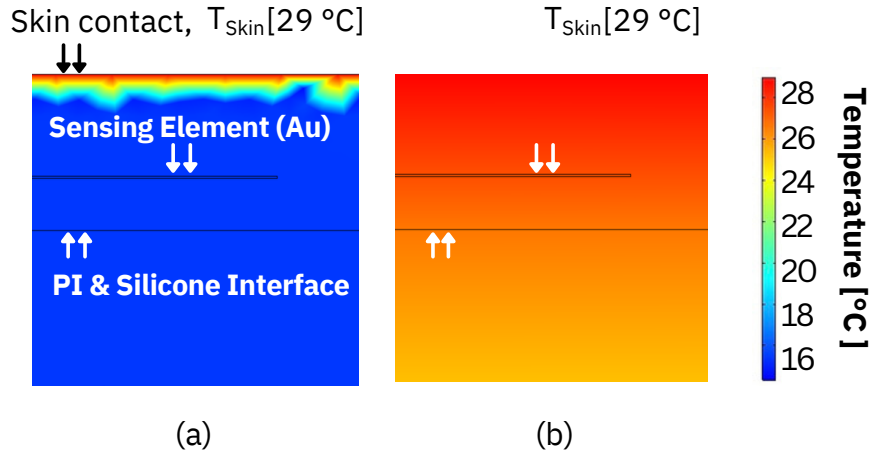
Figure 5.1: Temperature distribution across the cross section of the epidermal TCR sensor at a) t=0 ms b) t=3.9 ms.
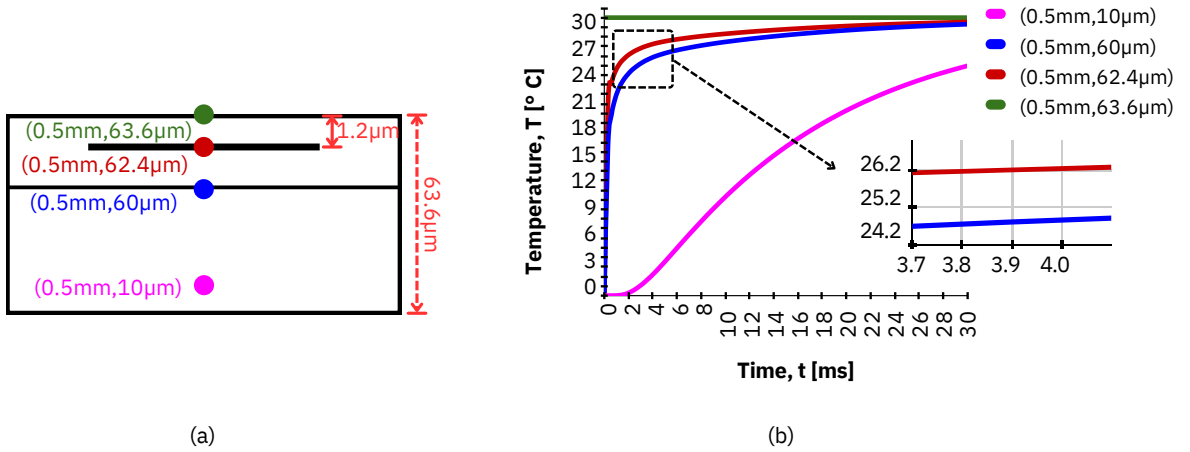

Figure 5.2: (a) Four points of observation across the cross-section of the epidermal TCR sensors and (b) time evolution of the corresponding temperature.
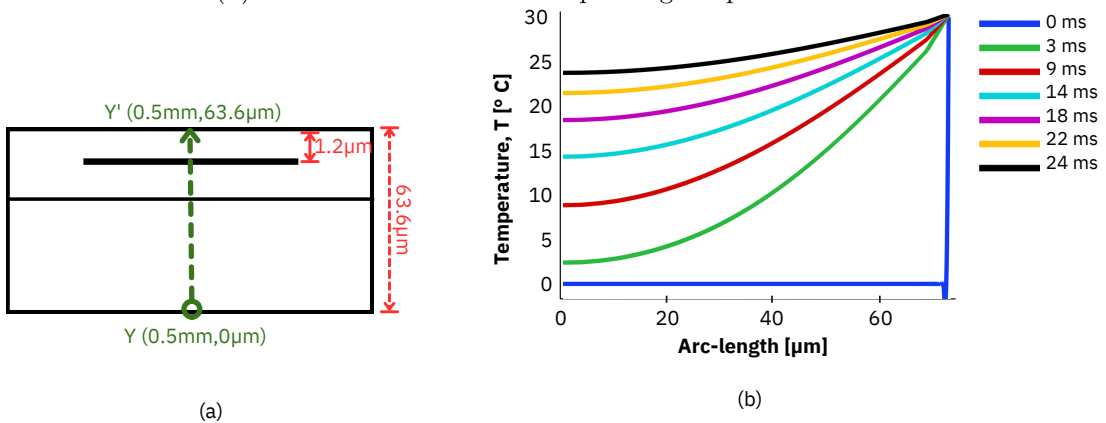

Figure 5.3: (a) A line YY' passing through the middle of the cross-section of the epidermal TCR sensor (b) temperature distribution along YY'.
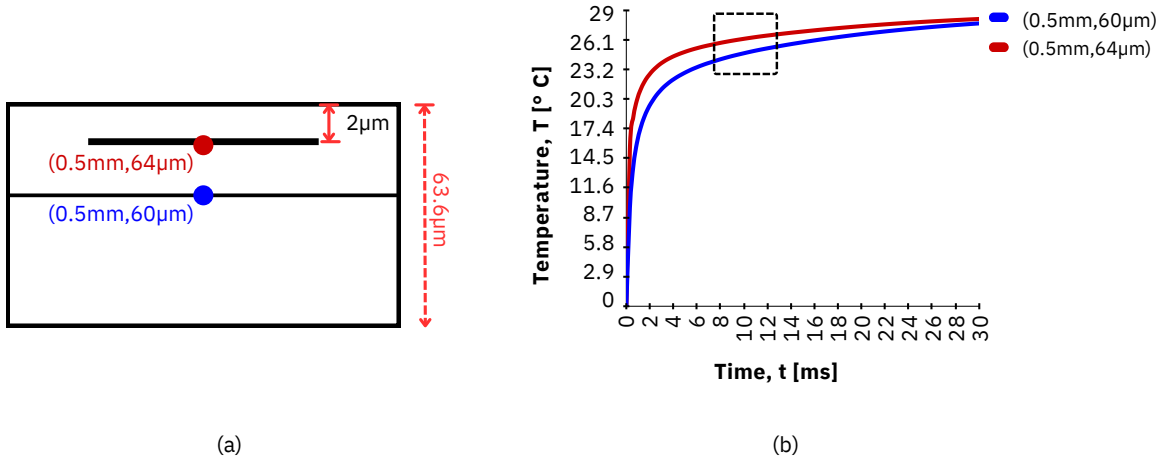
31

Figure 5.4: (a) Points defined at two locations for the case when encapsulation layer is increased from 1.2µm to 2µm (b) Shows corresponding increased response

5.2 IRKA results

Simulation time is chosen to be 30ms with time step of 0.3 and relative tolerance $1e^{-3}$. The interpolation points selected randomly and iteratively are used to build ROM while keeping the initial conditions zero for the original and reduced model both. Figure 5.5 is representing the transient response of the FOM and the ROM with different orders of reduction (r) and in Figure 5.6 the relative error can be seen w.r.t change in r. It is observed that the ROM generates output closely matching that of the original model except for r=5 where the output deviates largely from the original output. The simulation of FOM took approximately 48 sec while time taken to simulate the reduced model for r= 5, 15, 30 is 0.4891sec, 2.1788 sec and 6.5589 sec to compute the time response which was $\approx 3.9ms$ (Table 5.1). ROM simulates easily and quickly with less computational power ROM and is stable as well.

There are many ways to increase the accuracy of ROM and increasing reduction order is one of them but it will eventually increase simulation time. Figure **??** is showing relative error with respect to changing reduction order.

One important thing that should be noticed here is that the relative tolerance, time step, and time interval is set approximately same in COMSOL and MATLAB and both the simulations are carried out on a board with 11th Gen Intel(R) Core(TM) i7-11700, 32 GB RAM.
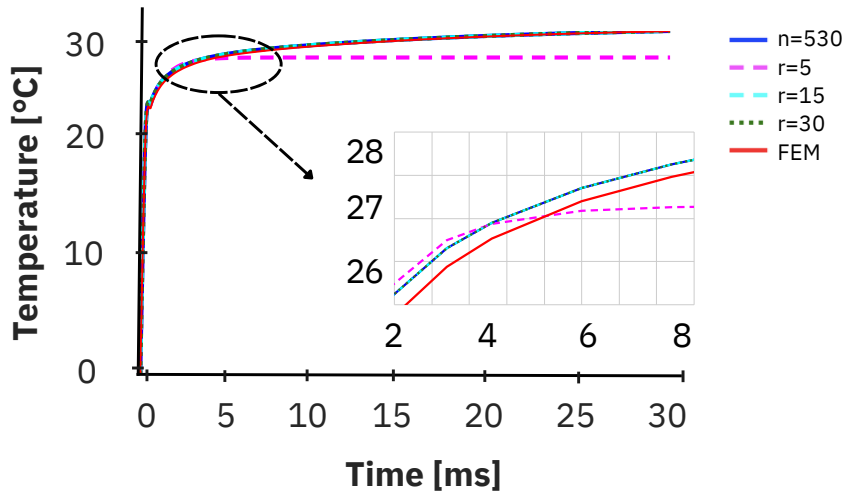
Figure 5.5: Temperature profile of FOM (n=530), FEM, and ROMs (r=5, 15, 30).
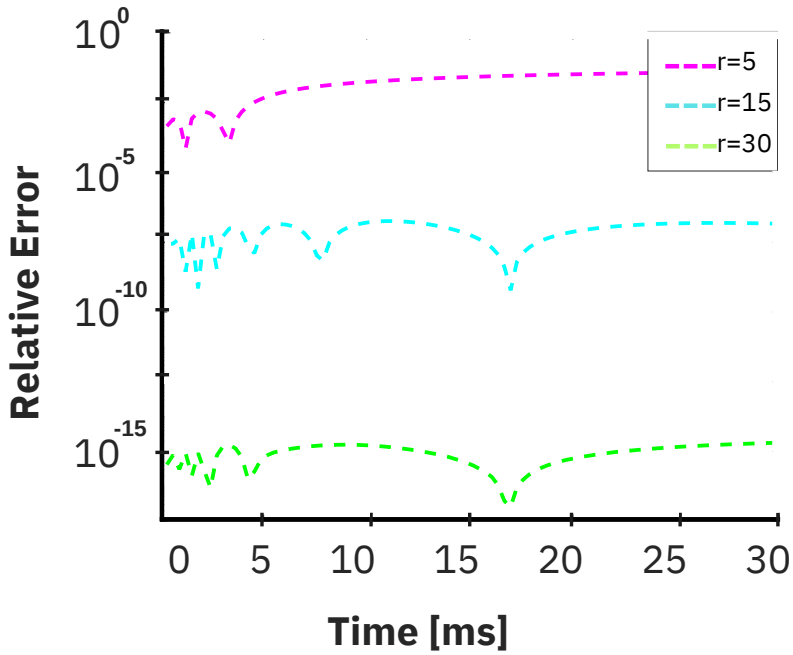

Figure 5.6: Relative errors for the three different orders of IRKA (r=5, 15 and 30) in modelling the time evolution of temperature of the TCR sensor with respect to full order model with n=530; the temperature is modelled within the gold sensing element at point (0.5mm, 62.4 μm as shown in Figure 5.

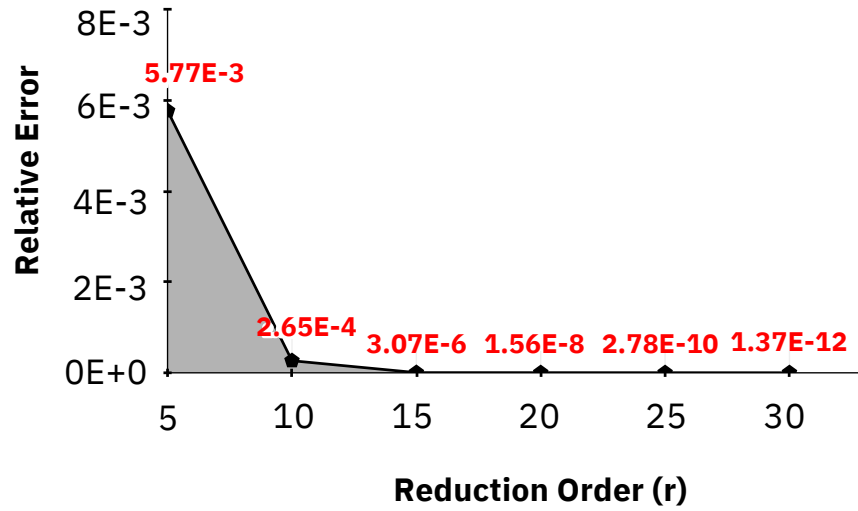**Figure 5.7:** Relative error with increase of reduction order (r).

	DEGREES OF FREEDOM	COMPUTATION TIME
FEM (COMSOL)	$\approx 68k$	40 min
FDM (MATLAB)	530	48 sec
IRKA	5	0.4891 sec
	15	2.1788 sec
	30	6.5589 sec

Table 5.1: Comparison Table

CHAPTER 6

Conclusion and future work

In this research, the Iterative Rational Krylov algorithm (IRKA) based MOR is used to model temperature distribution and response time of the epidermal TCR sensor. The main goal of applying IRKA was to reduce the computation time while keeping high accuracy, maintaining stability and quick sensor response time. We observed that FEM simulation took ≈ 40 minutes to model the sensor while after implementing IRKA of order r=30, the simulation was 3 orders faster and that as we increased the reduction order the more accurate results were achieved. This reduction of computation time will help the designers remarkably to perform iterative design processes more quickly and efficiently by utilising the smaller models instead of higher-order original models. Moreover, IRKA's potential for large computational savings lays the foundation for accurate and time efficient design of related systems especially in the field of biomedical where development of light weight sensors and probes is growing day by day. This will help for various design optimisations, parametric analyses, and real-time applications where computing speed is essential without compromising the precision.

6.1   Future work

Given that micro-level systems commonly consist of coupled subsystems, typically in array structures, it is preferable to breakdown each subsystem separately and couple them back together for system-level simulation. Therefore, for future work, we aim to find a certain type of compact thermal representation that makes coupling simple to the following thermal port while allowing heat fluxes to pass the boundaries. It is

uncertain how to combine the thermal fluxes at the shared surfaces between two finite element models in order to produce the thermal ports that would tie together a number of compact models.

Bibliography

[1]   Cornelius Lanczos. "An iteration method for the solution of the eigenvalue problem of linear differential and integral operators". In: (1950).

[2]   Cornelius Lanczos. "Solution of systems of linear equations by minimized iterations". In: *J. Res. Nat. Bur. Standards* 49.1 (1952), pp. 33–53.

[3]   E Davison. "A method for simplifying linear dynamic systems". In: *IEEE Transactions on automatic control* 11.1 (1966), pp. 93–101.

[4]   L. Meier and David G. Luenberger. "Approximation of linear constant systems". In: *IEEE Transactions on Automatic Control* 12 (1967), pp. 585–588.

[5]   MR Chidambara. "Two simple techniques for the simplification of large dynamic systems". In: *Joint Automatic Control Conference.* 7. 1969, pp. 669–674.

[6]   DA Wilson. "Optimum solution of model-reduction problem". In: *Proceedings of the institution of electrical engineers.* Vol. 117. 6. IET. 1970, pp. 1161–1165.

[7]   G Mahapatra. "A further note on selecting a low-order system using the dominant eigenvalue concept". In: *IEEE Transactions on Automatic Control* 24.1 (1979), pp. 135–136.

[8]   Bruce Moore. "Principal component analysis in linear systems: Controllability, observability, and model reduction". In: *IEEE transactions on automatic control* 26.1 (1981), pp. 17–32.

[9]   D. Hyland and D. Bernstein. "The optimal projection equations for model reduction and the relationships among the methods of Wilson, Skelton, and Moore". In: *IEEE Transactions on Automatic Control* 30.12 (1985), pp. 1201–1211. DOI: 10.1109/TAC.1985.1103865.

[10]   L.T. Pillage and R.A. Rohrer. "Asymptotic waveform evaluation for timing analysis". In: *IEEE Transactions on Computer-Aided Design of Integrated Circuits and Systems* 9.4 (1990), pp. 352–366. DOI: 10.1109/43.45867.

[11]   Axel Ruhe. "Rational Krylov algorithms for nonsymmetric eigenvalue problems. II. Matrix pairs". In: *Linear algebra and its Applications* 197 (1994), pp. 283–295.

[12]   Eric James Grimme. *Krylov projection methods for model reduction.* University of Illinois at Urbana-Champaign, 1997.

[13]   Roland W Freund. "Reduced-order modeling techniques based on Krylov subspaces and their use in circuit simulation". In: *Applied and Computational Control, Signals, and Circuits: Volume 1* (1999), pp. 435–498.

[14]   Wei-Yong Yan and James Lam. "An approximate approach to H2 optimal model reduction". In: *IEEE Trans. Autom. Control.* 44 (1999), pp. 1341–1358.

[15]   H.A. van der Vorst. "Krylov subspace iteration". In: *Computing in Science Engineering* 2.1 (2000), pp. 32–37. DOI: 10.1109/5992.814655.

[16]   Evgenii B Rudnyi and Jan G Korvink. "Automatic Model Reduction for Transient Simulation of MEMS-based Devices". In: *Sensors update* 11.1 (2002), pp. 3–33.

[17]   Jan G Korvink and Evgenii B Rudnyi. "Computer-aided engineering of electro-thermal MST devices: moving from device to system simulation". In: *Proc. EUROSIME.* Vol. 3. 2003.

[18]   Biswa Datta. *Numerical methods for linear control systems.* Vol. 1. Academic Press, 2004.

[19]   Jan Lienemann et al. "MEMS compact modeling meets model order reduction: Examples of the application of Arnoldi methods to microsystem devices". In: *the technical proceedings of the 2004 nanotechnology conference and trade show, Nanotech.* Vol. 4. Citeseer. 2004.

[20]   Athanasios C Antoulas. *Approximation of large-scale dynamical systems.* SIAM, 2005.

[21]   Tamara Bechtold. "Model order reduction of electro-thermal MEMS". PhD thesis. Freiburg (Breisgau), Univ., Diss., 2005, 2005.

[22]   Thilo Penzl. "Algorithms for model reduction of large dynamical systems". In: *Linear algebra and its applications* 415.2-3 (2006), pp. 322–343.

[23]   Valeria Simoncini and Daniel B Szyld. "Recent computational developments in Krylov subspace methods for linear systems". In: *Numerical Linear Algebra with Applications* 14.1 (2007), pp. 1–59.

[24]   Serkan Gugercin, Athanasios C. Antoulas, and Christopher A. Beattie. "H2 Model Reduction for Large-Scale Linear Dynamical Systems". In: *SIAM J. Matrix Anal. Appl.* 30 (2008), pp. 609–638.

[25]   Chin Leong Lim, Chris Byrne, and Jason KW Lee. "Human thermoregulation and measurement of body temperature in exercise and clinical settings". In: *Annals Academy of Medicine Singapore* 37.4 (2008), p. 347.

[26]   Wil Schilders. "Introduction to model order reduction". In: *Model order reduction: theory, research aspects and applications* (2008), pp. 3–32.

[27]   Wil Schilders. "Introduction to model order reduction". In: *Model order reduction: theory, research aspects and applications* (2008), pp. 3–32.

[28]   Mian Ilyas Ahmad. "Krylov subspace techniques for model reduction and the solution of linear matrix equations". In: (2011).

[29]   Theodore L Bergman. *Introduction to heat transfer.* John Wiley Sons, 2011.

[30]   Shankhadeep Das, Sanjay Mathur, and Jayathi Murthy. "Finite-Volume Method for Structural Analysis of RF MEMS Devices Using the Theory of Plates". In: *Numerical Heat Transfer* Part B: Fundamentals (Aug. 2012), pp. 1–21. DOI: 10.1080/10407790.2011.630949.

[31]   Farbod Khoshnoud and Clarence W de Silva. "Recent advances in MEMS sensor technology-mechanical applications". In: *IEEE Instrumentation & Measurement Magazine* 15.2 (2012), pp. 14–24.

[32]   Goro Obinata and Brian DO Anderson. *Model reduction for control system design.* Springer Science & Business Media, 2012.

[33]   SR Desai and Rajendra Prasad. "A novel order diminution of LTI systems using Big Bang Big Crunch optimization and Routh Approximation". In: *Applied Mathematical Modelling* 37.16-17 (2013), pp. 8016–8028.

[34]   Lihong Feng, Peter Benner, and Jan G Korvink. "System-Level Modeling of MEMS by Means of Model Order Reduction (Mathematical Approximations)–Mathematical Background". In: *System-Level Modeling of MEMS* (2013), pp. 53–93.

[35] Jizhou Song et al. "Ultrathin conformal devices for precise and continuous thermal characterization of human skin". In: (2013).

[36] Zuguang Bian et al. "Thermal analysis of ultrathin, compliant sensors for characterization of the human skin". In: *Rsc Advances* 4.11 (2014), pp. 5694–5697.

[37] Cristiano Henrique Gonçalves de Brito, Cristiana Brasil Maia, and José Ricardo Sodré. "A Mathematical Model for the Exhaust Gas Temperature Profile of a Diesel Engine". In: *Journal of Physics: Conference Series* 633 (2015).

[38] Ying Chen et al. "Breathable and stretchable temperature sensors inspired by skin". In: *Scientific reports* 5.1 (2015), p. 11505.

[39] Afzal Sikander and Rajendra Prasad. "Linear time-invariant system reduction using a mixed methods approach". In: *Applied Mathematical Modelling* 39.16 (2015), pp. 4848–4858.

[40] Yihui Zhang et al. "Theoretical and experimental studies of epidermal heat flux sensors for measurements of core body temperature". In: *Advanced healthcare materials* 5.1 (2016), pp. 119–127.

[41] Braid A MacRae et al. "Skin temperature measurement using contact thermometry: a systematic review of setup variables and their effects on measured values". In: *Frontiers in physiology* 9 (2018), p. 29.

APPENDIX A

IRKA Framework

Iterative Rational Krylov Algorithm [24]: Given a full-order $G(s)$, a reduction order r, and convergence tolerance tol.

1. Make an initial selection of r distinct interpolation points, $\{s_i\}_{i=1}^r$, that is closed under complex conjugation.

2. Construct $\boldsymbol{V}_r$ and $\boldsymbol{W}_r$

3. while (relative change in $\{s_i\} > tol$)

(a) $\boldsymbol{A}_r = \left(\boldsymbol{W}_r^T\boldsymbol{V}_r\right)^{-1}\boldsymbol{W}_r^T\boldsymbol{A}\boldsymbol{V}_r$

(b) Solve the $r \times r$ eigenvalue problem $\boldsymbol{A_r}\boldsymbol{u} = \boldsymbol{\lambda}\boldsymbol{u}$ and assign $s_i \leftarrow -\lambda_i\left(\boldsymbol{A}_r\right)$ for $i = 1, \ldots, r$.

(c) Update $\boldsymbol{V}_r$ and $\boldsymbol{W}_r$ with new s_i

4. $\boldsymbol{A}_r = \left(\boldsymbol{W}_r^T\boldsymbol{V}_r\right)^{-1}\boldsymbol{W}_r^T\boldsymbol{A}\boldsymbol{V}_r, \quad \boldsymbol{B}_r = \left(\boldsymbol{W}_r^T\boldsymbol{V}_r\right)^{-1}\boldsymbol{W}_r^T\boldsymbol{B}$, and $\boldsymbol{C}_r = \boldsymbol{V}_r^T\boldsymbol{C}$.